Evolutionary Computation of Supersonic Wing Shape Optimization

Shigeru Obayashi **Daisuke Sasaki** **Yukihiro Takeguchi**

Department of Aeronautics and Space Engineering, Tohoku University

Aoba-yama 01, Sendai, Japan 980-8579

Abstract

This paper discusses design optimization of a wing for supersonic transport (SST) using Multiple Objective Genetic Algorithm (MOGA). Three objective functions are used to minimize the drag for supersonic cruise, the drag for transonic cruise and the bending moment at the wing root for supersonic cruise. The wing shape is defined by in total of 66 design variables. An Euler flow code is used to evaluate supersonic performance, and a potential flow code is used to evaluate transonic performance. To reduce the total computational time, flow calculations are parallelized on NEC SX-4 computer using 32 PE's. The detailed analysis of the resulting Pareto front suggests a renewed interest in the arrow wing planform for the supersonic wing.

1 INTRODUCTION

To respond future increase of air traffic demand, development of next generation supersonic transport is considered worldwide. Aerodynamic design of such aircraft must account for drag reduction as well as sonic boom minimization. However, drag reduction is in conflict with sonic boom minimization. Since acceptability of supersonic transport is very sensitive to the sonic boom over populated areas, one of the design choices is to limit supersonic flight over sea and to have transonic flight over land. Although such decision excludes the sonic boom from the design consideration, the design is now faced with transonic performance of the aircraft.

This paper considers multipoint aerodynamic optimization of a wing shape for supersonic aircraft both at a supersonic cruise condition and at a transonic cruise condition. Aerodynamic drag will be minimized at both cruise conditions under lift constraints. Aerodynamic optimization of the wing planform, however, drives the wing to have an impracticably large aspect ratio. Therefore, minimization of the wing root bending moment is added as a third design objective.

The present multipoint design problem can be regarded as multiobjective (MO) optimization. Solutions to MO problems are often computed by combining multiple criteria into a single criterion according to some utility function. In many cases, however, the utility function is not well known prior to the optimization process. The whole problem should then be treated with non-commensurable objectives. MO optimization seeks to optimize the components of a vector-valued objective function. Unlike single objective optimization, the solution to this problem is not a single point, but a family of points known as the Pareto-optimal set.

By maintaining a population of solutions, Genetic Algorithms (GA) can search for many Pareto-optimal solutions in parallel. This characteristic makes GAs very attractive for solving MO problems. As a solver for MO problems, the following two features are desired: 1) the solutions obtained are Pareto-optimal and 2) they are uniformly sampled from the Pareto-optimal set. To achieve these, MOGAs have successfully been introduced by Fonseca and Fleming, 1993.

Furthermore, it was shown that the so-called best-N selection helps to find the extreme Pareto solutions (Obayashi, Takahashi and Takeguchi, 1998). The best-N selection picks up the best N individuals among N parents and N children for the next generation similar to CHC (Eshelman, 1991). The extreme Pareto solutions are the optimal solutions of the single objectives. By examining the extreme Pareto solutions, quality of Pareto solutions can be measured. The present MO problem will be solved by using MOGA coupled with the best-N selection.

2 APPROACH

In GAs, the natural parameter set of the optimization problem is coded as a finite-length string. Traditionally, GAs use binary numbers to represent such strings: a string has a finite length and each bit of a string can be either 0 or 1. For real function optimization, however, it is more natural to use real numbers. The length of the real-number string corresponds to the number of design variables.

2.1 CROSSOVER AND MUTATION

A simple crossover operator for real number strings is the average crossover (Davis, 1990) which computes the

arithmetic average of two real numbers provided by the mated pair. In this paper, a weighted average is used as

$$\text{Child1} = ran1\cdot\text{Parent1} + (1-ran1)\cdot\text{Parent2}$$
$$\text{Child2} = (1-ran1)\cdot\text{Parent1} + ran1\cdot\text{Parent2} \quad (1)$$

where Child1,2 and Parent1,2 denote encoded design variables of the children (members of the new population) and parents (a mated pair of the old generation), respectively. The uniform random number *ran*1 in [0,1] is regenerated for every design variable.

Mutation takes place at a probability of 20% (when a random number satisfies *ran*2 < 0.2) initially and the rate is going to decline linearly during the evolution. Equations (1) will then be replaced by

$$\text{Child1} = ran1\cdot\text{Parent1} + (1-ran1)\cdot\text{Parent2} + m\cdot(ran3-0.5)$$
$$\text{Child2} = (1-ran1)\cdot\text{Parent1} + ran1\cdot\text{Parent2} + m\cdot(ran3-0.5) \quad (2)$$

where ran2 and ran3 are also uniform random numbers in [0,1] and m determines the range of possible mutation.

2.2 MULTIOBJECTIVE PARETO RANKING

To search Pareto-optimal solutions by using MOGA, the ranking selection method (Goldberg, 1989) can be extended to identify the near-Pareto-optimal set within the population of GA. To do this, the following definitions are used: suppose $\mathbf{x}_i$ and $\mathbf{x}_j$ are in the current population and $\mathbf{f} = (f_1, f_2, \cdots, f_q)$ is the set of objective functions to be maximized,

1. $\mathbf{x}_i$ is said to be dominated by (or inferior to) $\mathbf{x}_j$, if $\mathbf{f}(\mathbf{x}_i)$ is partially less than $\mathbf{f}(\mathbf{x}_j)$, i.e., $f_1(\mathbf{x}_i) \le f_1(\mathbf{x}_j) \wedge f_2(\mathbf{x}_i) \le f_2(\mathbf{x}_j) \wedge \cdots \wedge f_q(\mathbf{x}_i) \le f_q(\mathbf{x}_j)$ and $\mathbf{f}(\mathbf{x}_i) \ne \mathbf{f}(\mathbf{x}_j)$.
2. $\mathbf{x}_i$ is said to be non-dominated if there doesn't exist any $\mathbf{x}_j$ in the population that dominates $\mathbf{x}_i$.

Non-dominated solutions within the feasible region in the objective function space give the Pareto-optimal set.

Let's consider the following optimization:

Maximize: $f_1 = x,\ f_2 = y$

Subject to: $x^2 + y^2 \le 1$ and $0 \le x, y \le 1$

The Pareto front of the present test case becomes a quarter arc of the circle $x^2 + y^2 = 1$ at $0 \le x, y \le 1$.

Consider an individual $\mathbf{x}_i$ at generation t (Fig. 1) which is dominated by p_i^t individuals in the current population. Following Fonseca and Fleming (1993), its current position in the individuals' rank can be given by

$$\text{rank}(\mathbf{x}_i, t) = 1 + p_i^t \quad (3)$$

All non-dominated individuals are assigned rank 1 as shown in Fig. 1. The fitness values are reassigned according to rank as an inverse of their rank values. Then the SUS method (Baker, 1987) takes over with the reassigned values.

2.3 FITNESS SHARING

To sample Pareto-optimal solutions from the Pareto-optimal set uniformly, it is important to maintain genetic diversity. It is known that the genetic diversity of the population can be lost due to the stochastic selection process. This phenomenon is called the random genetic drift. To avoid such phenomena, the niching method has been introduced (Goldberg, 1989).

The model used here is called fitness sharing (FS). A typical sharing function is given by Goldberg (1989). The sharing function depends on the distance between individuals. The distance can be measured with respect to a metric in either genotypic or phenotypic space. A genotypic sharing measures the interchromosomal Hamming distance. A phenotypic sharing can further be classified into two types. One measures the distance between the decoded design variables. The other, on the other hand, measures the distance between the designs' objective function values. Here, the latter phenotypic sharing is employed since we seek a global tradeoff surface in the objective function space.

This scheme introduces new GA parameters, the niche size σ_{share}. The choice of σ_{share} has a significant impact on the performance of MOGAs. Fonseca and Fleming (1993) gave a simple estimation of σ_{share} in the objective function space as

$$N\sigma_{share}^{q-1} - \frac{\prod_{i=1}^{q}(M_i - m_i + \sigma_{share}) - \prod_{i=1}^{q}(M_i - m_i)}{\sigma_{share}} = 0 \quad (4)$$

where N is a population size, q is a dimension of the objective vector, and M_i and m_i are maximum and minimum values of each objective, respectively. This formula has been successfully adapted here. Since this formula is applied at every generation, the resulting σ_{share} is adaptive to the population during the evolution process. Niche counts can be consistently incorporated into the fitness assignment according to rank by using them to scale individual fitness within each rank.

3 RESULTS

Flow conditions are M_∞ = 2.0 and C_L = 0.1 for supersonic cruise and M_∞ = 0.9 and C_L = 0.15 for transonic cruise. The supersonic inviscid drag to be minimized is evaluated by using an Euler flow solver (Obayashi et al. 1998). The transonic inviscid drag is evaluated by using a full potential flow solver (Jameson and Caughey, 1977). The bending moment is evaluated by directly integrating the pressure load at the supersonic cruise condition.

Design variables are illustrated in Figs. 2-5. The wing planform is determined by six design variables as shown in Fig. 2. The variable ranges are summarized in Table 1. A wing area is fixed at $S = 60$. A chord length at the wing tip is automatically determined due to the given wing area. An airfoil shape is defined by its thickness distribution and camber line. The thickness distribution is given by a Bezier curve shown in Fig. 3. The maximum thickness is constrained from 3 % to 4 % chord lengths. The location of the maximum thickness is also constrained from 15 % to 70 % chordwise locations. The thickness distributions are defined at the wing root, kink and tip. They are linearly interpolated in the spanwise direction. The camber surfaces are defined at the inboard and outboard of the wing separately. Each surface is given by the Bezier surface using four polygons in the chordwise direction and three polygons in the spanwise direction. The resulting camber line at the wing root is shown in Fig. 4. It is concave only at the root and it becomes convex at the other spanwise locations similar to the linearized theory. Finally, the wing twist is defined by a B-spline curve as shown in Fig. 5. A monotonic variation is enforced by rearranging the polygons in numerical order in the spanwise direction. In total, 66 design variables are used.

MOGA is used as a design optimizer. Flow calculations were parallelized on 32 PE's of NEC SX-4 computer at Computer Center of Tohoku University, using the simple *Master-Slave* concept. The population size was set to 64 and 70 generations were run. To constrain the lift coefficient, three flow calculations were used per drag evaluation. The total computational time was roughly 100 hours.

Figure 6 shows the resulting Pareto solutions in the three dimensional objective function space. They form an approximate tradeoff surface. Typical planform shapes are also plotted in the figure. The extreme Pareto solutions (denoted as bending moment minimum, C_D(supersonic) minimum, C_D(transonic) minimum) have physically reasonable shapes: a very short span length (corresponding to a large taper ratio as well as a low aspect ratio) for minimizing bending moment, high aspect ratios for minimizing induced drag and larger sweep angles for minimizing wave drag. These results indicate the validity of the present optimization.

Tradeoffs between the objectives can be observed more easily in the two-dimensional projections as shown in Figs. 7 and 8. Figure 7 presents the tradeoffs between supersonic and transonic drag coefficients. The Pareto solutions are plotted in different symbols according to the aspect ratio. Lower drag coefficients are obtained from larger aspect ratios in general as suggested by the standard aerodynamic theory.

In Fig. 7, the edge of the projected Pareto surface I indicates purely aerodynamic tradeoffs between supersonic and transonic flights. This curve would be the Pareto front if only these two objectives are used. However, as shown in Fig. 6, the extreme Pareto solutions for supersonic and transonic drag have too large aspect ratios, and thus they are impossible to be built within a reasonable structural weight. This is true for all solutions on the edge I. The other edge of the projected Pareto surface II indicates the tradeoffs between the supersonic drag and the bending moment. (Note that the bending moment is evaluated at the supersonic flight condition.) A practical wing shape is expected to appear in this region.

Figure 8 illustrates the tradeoffs between the bending moment and the supersonic drag. The edge of the projected Pareto surface forms a simple convex curve toward the lower left corner of the figure, representing the pure tradeoffs between these two objectives. The edge IV may be less interesting to aircraft designers because it indicates severe penalties in the drag with little improvements in the bending moment. On the other hand, the edge III represents more reasonable tradeoffs. The Pareto solutions are plotted in different symbols according to the taper ratio. To be on the edge III, the taper ratio of the wing should roughly be less than 0.4.

To evaluate the present Pareto solutions further, they are compared with the aerodynamic design of the supersonic wing for National Aerospace Laboratory's Scaled Supersonic Experimental Airplane (Iwamiya, 1998). NAL SST Design Team has performed the following four aerodynamic designs. The first design was a selection of a planform shape among 99 different shapes by direct comparisons. The second design was performed by the warp optimization based on the linearized theory. The third design was obtained from an inverse design to yield a natural laminar flow based on the Navier-Stokes code. The fourth design was then performed for a wing-fuselage configuration. Since the present optimization is based on the inviscid flow codes, NAL's second design is chosen for the comparison here. Its performance was evaluated by using the same codes in this study.

Figure 9 and Table 2 summarize the comparisons of six Pareto solutions with NAL's second design. It should be noted that NAL's design appears close to the edge II in Fig. 7. This indicates that the edge II represents practical solution area as well as that the warp optimization of NAL's design has a good accuracy. Six solutions were picked up so as to represent the sensitivity of the Pareto surface. The solutions A, B and C have transonic drag similar to NAL's design but their supersonic drag is in order of A < B < C. (The solution C and NAL's design perform alike.) To improve the supersonic performance over NAL's design, the taper ratio of the wing becomes larger and the root chord length becomes smaller. However, there is an upper limit for the taper ratio from the observation in Fig. 8.

The solutions C, D and E have supersonic drag similar to NAL's design and transonic drag in order of E < D < C. To improve the transonic performance over NAL's design, the aspect ratio of the wing becomes larger and the root chord length becomes smaller. However, the increase of the aspect ratio also results in the increase of the bending moment as indicated in Table 2.

Finally, the solution F is found to outperform NAL's design in all three objectives. A common geometric feature among the three solutions A, E and F is their root chord lengths shorter than the root of NAL's design. This means that they have larger taper ratios. Aerodynamic theory generally suggests an increase of the aspect ratio to improve the aerodynamic performance as mentioned before. However, the present solution A, E and F all have smaller aspect ratios than NAL's design does. The resulting shape is somehow similar to the "arrow wing" planform rather than the conventional "delta wing" planform.

The arrow wing shape was originally derived from research in the late 1950's indicating that the optimum wing planform would be a highly swept, highly tapered, arrowhead shape (Nelson, 1992). Attempts to incorporate such arrow wing shapes eventually failed due to design integration difficulties, aeroelastic problems and high structural weight. Studies from 1970 to 80's then resulted in the "cranked arrow" wing. The cranked arrow retains the original arrow on inboard wing only. The "cranked" forward outboard wing provides more span and higher effective aspect ratio (Fig. 10). The main interest in the supersonic wing development has been an increase of the aspect ratio in compromise with the highly swept planform.

The present results suggest a new type of the arrow wing planform having a larger taper ratio instead of a larger aspect ratio. This means a less tapered arrow wing in contrast to the original, highly tapered arrow wing as compared in Fig. 10. In the present MOGA result, either the cranked arrow or the modified delta did not survive as a Pareto solution. The original arrow wing was abandoned due to the structural problems. After 40 years of the development in the structural dynamics and materials, the present arrow wing may be interesting for further studies.

4 CONCLUSIONS

The multipoint design optimization of a wing for SST has been performed by using MOGA. The three objective functions are used to minimize the drag for supersonic cruise, the drag for transonic cruise and the bending moment at the wing root for supersonic cruise. The wing shape is defined by in total of 66 design variables.

Physically reasonable extreme Pareto solutions were obtained from the present formulation. This indicates the validity of the present optimization. One of the Pareto solutions was found to outperform the existing design in all design objectives. The detailed analysis of the Pareto solutions suggests a new type of the arrow wing with a larger taper ratio and a smaller aspect ratio compared with the existing planform shapes.

Acknowledgments

This research was funded by Japanese Government's Grants-in-Aid for Scientific Research, No. 10305071. The first author's research has been partly supported by Bombardier Aerospace, Toronto, Canada. The computational time was provided by Computer Center, Tohoku University. The authors would like to thank National Aerospace Laboratory's SST Design Team for providing many useful data.

References

Baker, J. E. (1987) Reducing bias and inefficiency in the selection algorithm. *Proceedings of the Second International Conference on Genetic Algorithms*, 14-21. San Mateo, Calif.: Morgan Kaufmann Publishers.

Davis, L. (1990) Handbook of Genetic Algorithms, Reinhold, New York: Van Nostrand.

Eshelman, L. J. (1991) The CHC Adaptive Search Algorithm: How to Have Safe Search When Engaging in Nontraditional Genetic Recombination. *Foundations of Genetic Algorithms*, 265-283. San Mateo, Calif.: Morgan Kaufmann Publishers.

Fonseca, C. M. and Fleming, P. J. (1993) Genetic algorithms for multiobjective optimization: formulation, discussion and generalization. *Proceedings of the 5th International Conference on Genetic Algorithms*, 416-423. San Mateo, Calif.: Morgan Kaufmann Publishers.

Goldberg, D. E. (1989) *Genetic Algorithms in Search, Optimization & Machine Learning*. Reading, Mass.: Addison-Wesley.

Iwamiya, T. (1998) NAL SST Project and Aerodynamic Design of Experimental Aircraft, *Proceedings of the Fourth ECCOMAS Computational Fluid Dynamics Conference*, Vol. 2, 580-585. Chichester, UK: John Wiley & Sons.

Jameson, A. and Caughey, D. A. (1977) A Finite Volume Method For Transonic Potential Flow Calculations. AIAA paper 77-677. Reston, VA: American Institute of Aeronautics and Astronautics.

Nelson, C. P. (1992) Effects of Wing Planform on HSCT Off-Design Aerodynamics. AIAA paper 92-2629-CP. Reston, VA: American Institute of Aeronautics and Astronautics.

Obayashi, S., Nakahashi, K., Oyama, A. and Yoshino, N. (1998) Design Optimization of Supersonic Wings Using Evolutionary Algorithms. *Proceedings of the Fourth ECCOMAS Computational Fluid Dynamics Conference*, 575-579. Chichester, UK: John Wiley & Sons.

Obayashi, S., Takahashi, S. and Takeguchi, Y. (1998) Niching and Elitist Models for MOGAs. *Parallel Problem Solving from Nature - PPSN V*, 260-269, Lecture Notes in Computer Science. Berlin, Germany: Springer.

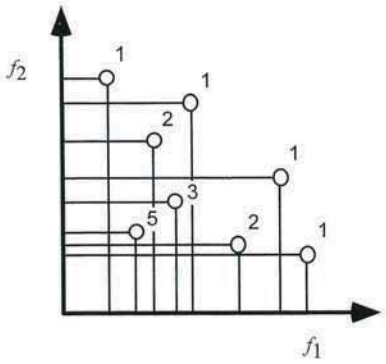

Figure 1: Pareto Ranking Method

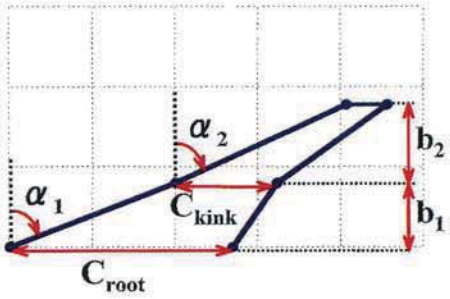

Figure 2: Wing Planform Definition

Table 1: Variable Domain for Planform Definition

Variable	Range
α_1	35 - 70 deg
α_2	35 - 70 deg
C_{root}	10 - 20
C_{kink}	3 - 5
b_1	2 - 7
b_2	2 -7

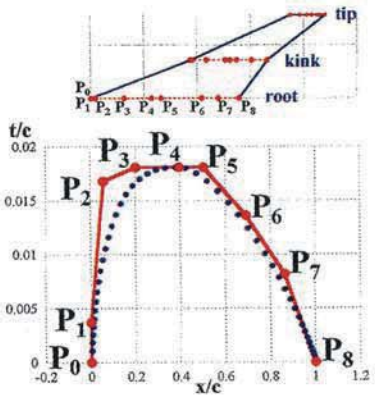

Figure 3: Wing Thickness Definition

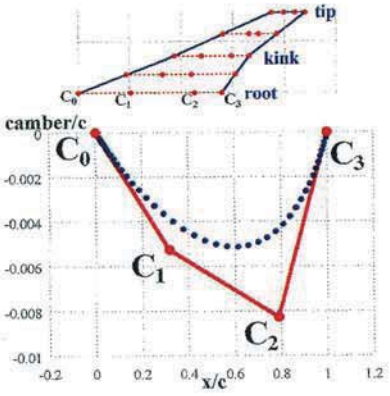

Figure 4: Wing Camber Definition

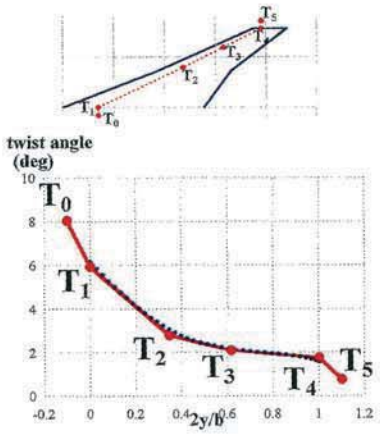

Figure 5: Wing Twist Definition

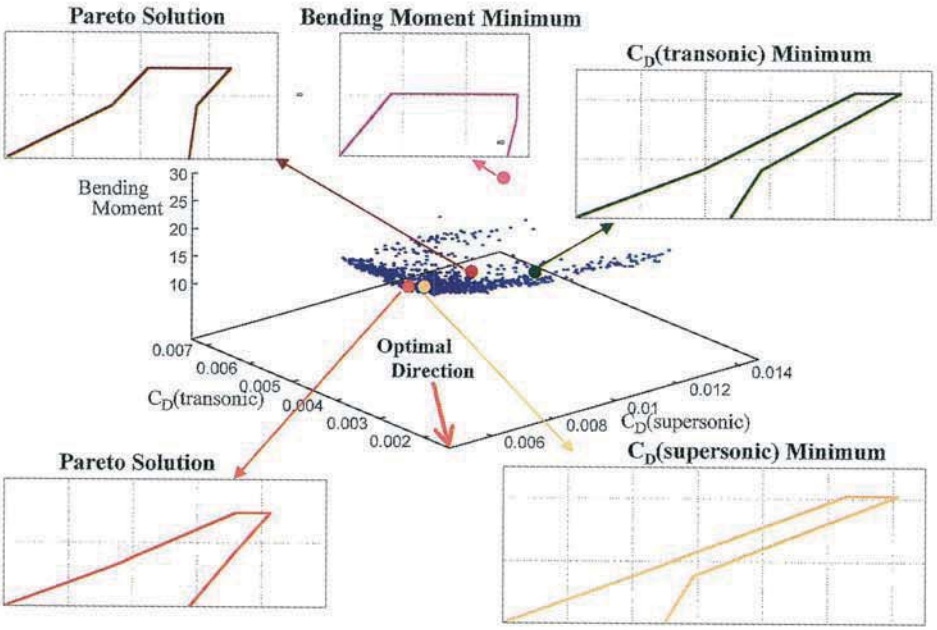

Figure 6: Pareto Front in the Objective Function Space and Typical Planform Shapes

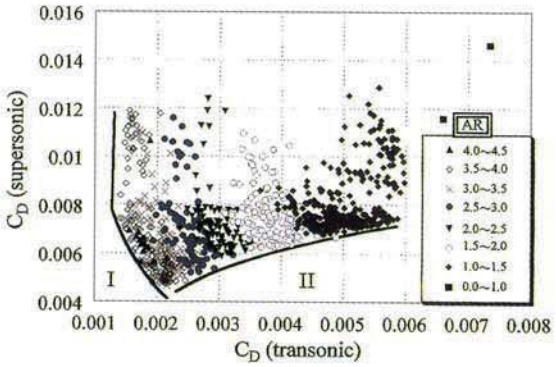

Figure 7: Projection of Pareto Front to Supersonic and Transonic Drag Tradeoffs

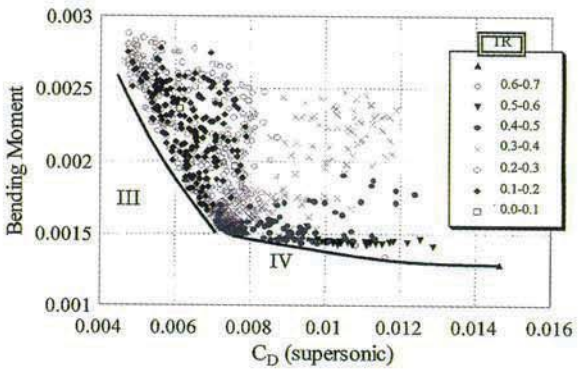

Figure 8: Projection of Pareto Front to Bending Moment and Supersonic Drag Tradeoffs

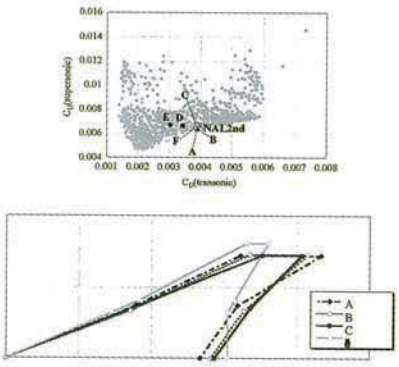

a) Pareto Solutions at Nearly Constant Transonic Drag

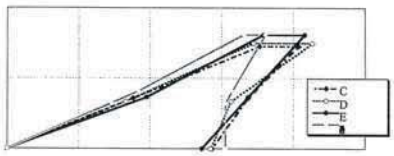

b) Pareto Solutions at Nearly Constant Supersonic Drag

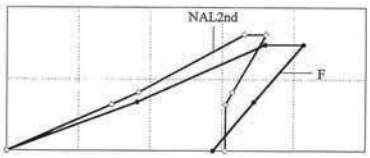

c) Pareto Solution Better Than NAL Design in All Three Objectives

Figure 9: Comparison of Pareto Solutions with NAL Inviscid Design